Journal of Machine Engineering, Vol. 14, No. 3, 2014

contact mechanics,
asperity deformation,
measurement

Pawel MACIOLKA[1]
Jerzy JEDRZEJEWSKI[1]
Miroslaw GROCHOWSKI[1]

A DEVICE FOR THE EXPERIMENTAL INVESTIGATION OF SURFACE CONTACT UNDER LOAD

The structure of a device for the investigation of the contact deformations of flat surfaces under normal load is described. The conditions, for which the device must satisfy in order to ensure normal load are defined. Errors which may occur during the loading of a rough specimen, relating to the mechanical structure of the device, the specimen itself and the measuring systems, are estimated. Finally, the device is subjected to testing which includes specimen roughness measurements before and after loading, the loading and unloading of the specimens in the device and again measuring their roughness. The device developed herein can be characterised by its vacuum mounting method of the specimen and also by the accurate and simple loading mechanism, i.e., movable member.

1. INTRODUCTION

In order to determine the proximity between two flat planes and to measure their roughness parameters one must identify in detail the mechanism of asperity deformation under load. The deformation of asperities in the joints between machine assemblies may have either clearly negative or insignificant consequences for the static and dynamic behaviour of the assemblies in the operating conditions. The adverse effects may include: local deformations of the parts [1] and a change in their geometry as well as changes in: the mutual position of the contacting surfaces [2],[3], the friction conditions [4], the thermal conductivity of the contact [5],[6], the electrical resistance of the contact and the wear resistance of the parts [7],[8]. A deformation is of little significance for the static and dynamic behaviour of a machine assembly when it is within the allowable range and does not cause negative effects. This may be the case when vibrations are to be damped.

There are many papers dealing with the investigation of the properties of the contact. Among the methods described in them one can distinguish three basic methods. The first method, based on statistics and the Greenwood-Willianson theory, consists in the use of statistical parameters for the description of a rough surface and the Hertz theory for the description of the deformations of individual asperities and for the approximation of their

[1] Wroclaw University of Technology, Institute of Production Engineering and Automation, Wroclaw, Poland
E-mail: pawel.maciolka@pwr.edu.pl

shape by means of a sphere or a hyperboloid [9],[10],[11]. The second method is based on the theory of fractals [12] and consists in describing the contact properties by means of the parameters and characteristics of fractals. The third method describes the interaction between surfaces by mapping the actual asperities by means of an FEM numerical model [13],[14],[15]. As regards the latter method, the highly advanced analyses of the contact, based on multiscale [16] and three-dimensional models of surface asperities [14],[15] deserve attention. They require data from three-dimensional measurements of asperities [13].

Regardless of its complexity, each model needs to be experimentally verified, which in the case of asperities of μm (and even fractions of μm) magnitude is technically difficult. In experimental studies constant conditions and stable contact parameters are often achieved through the use of a point load exerted by spherical surfaces [17],[18]. However, even more often there is a need to use two flat surfaces, which entails a considerable increase in the complexity of both the description of the contact and the experimental conditions for the verification of this description. The high requirements set for experimental investigations apply to the contact loading conditions, the surface characteristics of the specimens and the measuring stand design. The subsequent chapters are devoted to the above problems and to the testing of the measuring stand.

2. MEASURING STAND

A schematic of the measuring stand is shown in Fig. 1. The main components of the stand are: load-bearing structure (1) with movable member (7) and base (2), drive system (3) for moving punch (4) loading the specimen, loading block (5) with table (6), specimen (8) and measuring-monitoring units.

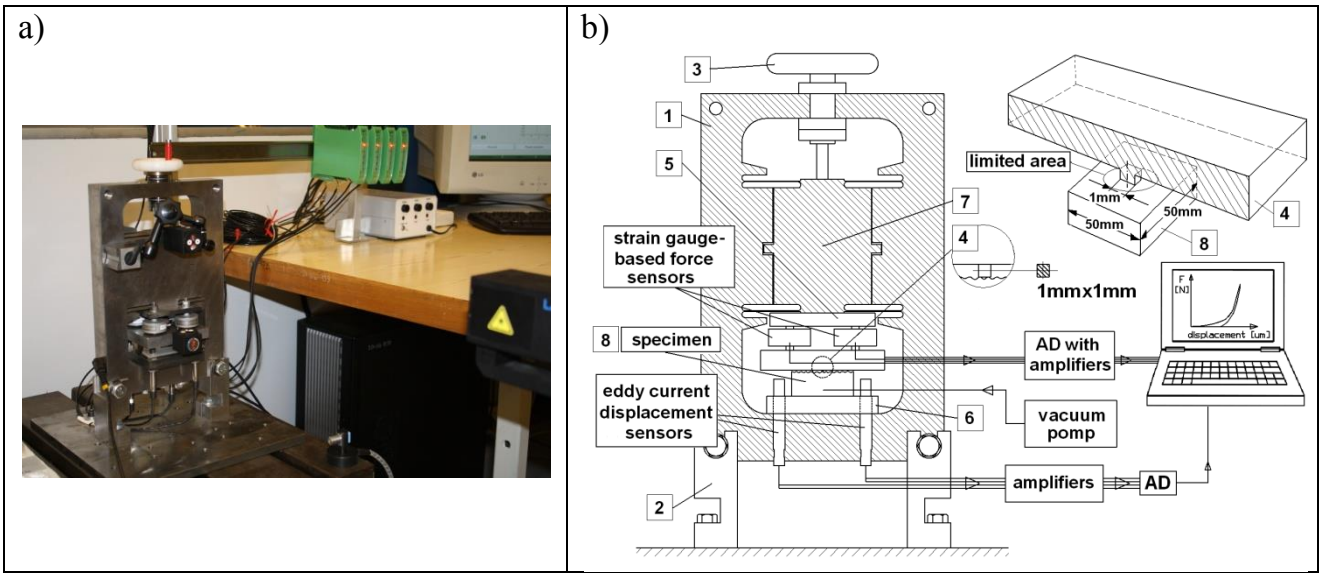

Fig. 1. View of measuring stand a), schematic of measuring stand b)

Load-bearing structure with base

The load-bearing structure is a monolithic frame with a movable internal member. It was made as a whole using the electro-erosion technique. The load-bearing structure is vertically fixed to the base. The movable internal member is suspended from elastically deformable slender structural members (Fig. 4) enabling its movement in the normal direction. The internal part can displace in the vertical direction within a range of +/-1.5mm. This load-bearing structure design was dictated by the need to ensure the smallest possible loading force deviations from the normal direction during the measurement process.

Drive system

A screw installed in the movable member of the frame and passing through a threaded rotary sleeve constitutes the drive system. The sleeve is mounted on ball bearings in the upper part of the frame. The vertical displacement of the movable member of the load-bearing structure is effected by manually turning a wheel connected with the sleeve. Thanks to this solution the movable member is unlikely to undergo deformations which would adversely affect the correctness of the contact characteristic being determined.

Loading block with table

Two hardened plates, with four sensors measuring the quantities and monitoring the direction of the force exerted on the tested specimen installed between them, form the loading block. The upper plate is fixed to the movable part of the frame while the lower plate is a punch for exerting load on the specimen. The punch has a protruding element in the form of a quadratic prism with a square cross section 1 mm^2 in area. According to ISO25178, the roughness parameters of this surface are: S_a=0.1322μm, S_z=4.727μm (S_a – the arithmetic mean height, S_z – the maximum height of the surface). By inserting a specimen between the loading block and the table the former can be lifted by 1.5mm. The table on which the specimen rests was ground and fixed to the frame. Four sensors for measuring the displacements of punch 4 relative to table 6 were set in it.

Specimens with system of vacuum channels

Two types of 50x50x19.5mm specimens were prepared for testing the measuring stand. The specimens in the first group were made of aluminium alloy EN AW-5754 and milled. They were characterized by high roughness (S_a=5.36μm, S_z=24.26μm acc. to ISO25178) and were used to evaluate the correctness of the determined proximity characteristic.

Because of the high stiffness of the specimen-punch contact the specimens forming the second group, characterized by considerably lower roughness (S_a=0.20μm, S_z=2.69μm), , were used to evaluate the properties of the device structure. They were made of steel NC10 with hardness 58HRC and subjected to grinding. The profilograms of the surface for the two types of specimens: a milled aluminium specimen and a ground steel specimen are shown in Fig. 2.

The vacuum fixing of the specimen in the device (Fig. 3) was used to minimize errors which may arise due to the incomplete adherence of the specimen to the table surface. A vacuum pump connected to a channel made in the bottom surface of the specimen is used to produce negative pressure under the specimen (the yellow colour) within the area limited by another channel in which a seal is set (the red colour).

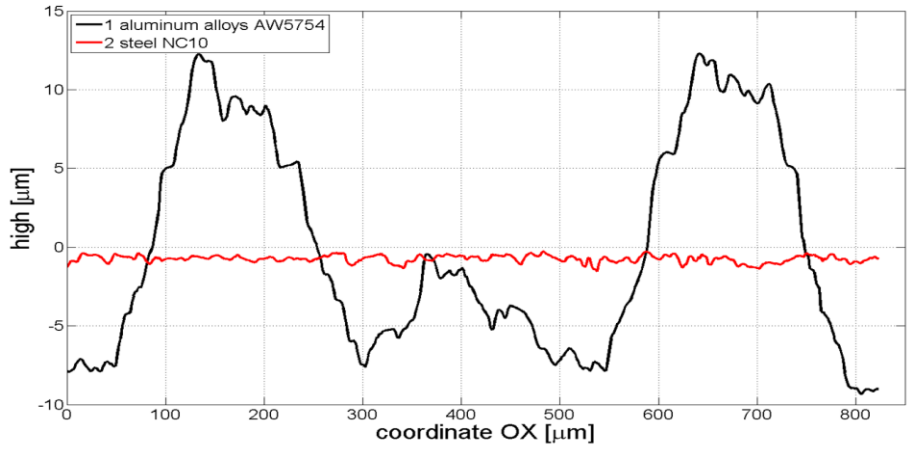

Fig. 2. Comparison of roughness profiles for respectively milled and ground specimens. Arithmetic mean height, S_a: 5. 36 (milled) and 0.2 (ground), maximum surface height, S_z: 24.26 (milled) and 2.69 (ground).

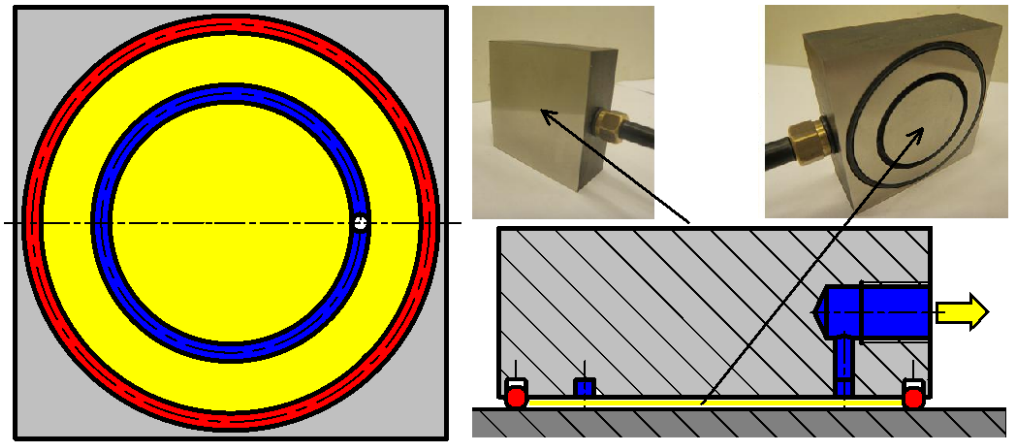

Fig. 3. Specimens with system of channels for producing vacuum

Measuring-monitoring system

The measuring-monitoring system consists of four eddy-current non-contacting displacement sensors and four strain gauge-based force sensors, which work together with power-supply systems, measuring cards and a computer with the LabView software. The arrangement of the force sensors and the displacement sensors, forming sensor pairs No. 1, No. 2, No. 3 and No.4 is shown in Fig. 4.

3. ANALYSIS OF REQUIREMENTS AND ACCURACY

The requirements for experimental investigations pertain to the characteristics of the surface of the samples, the measuring stand design, the place and direction of contact loading and roughness measurements by means of a profilometer.

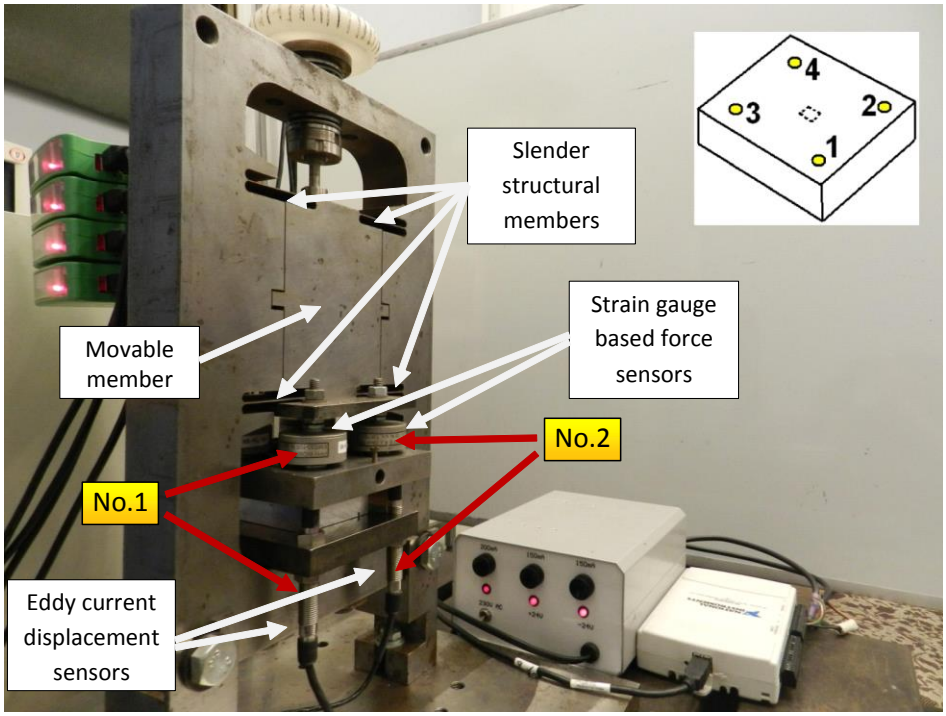

Fig. 4. Force-displacement sensor pairs in measuring stand

The surface characteristics limited to the roughness and material of the specimen impose requirements as to the design of the stand and its measuring capabilities. The first requirement applies to the displacement measuring range and measurement resolution, according to which the stand should enable the measurement of displacements with a resolution in the order of decimal fractions of μm in a range from a few nm to tens of μm. This requirement was satisfied through the choice of precision displacement sensors and an AD converter. Another requirements concerns the dependences between load values and asperity deformations. According to this requirement, the stand should be able of producing a large plastic deformation in the investigated contact at low load values, not exceeding 500N. This was achieved by limiting the nominal punch surface area to 1mm^2 and using specimens made of a compliant material, i.e. aluminium alloy. The milled aluminium specimens have a sufficiently high surface roughness in the order of tens of micrometers. Therefore it is easy to locate a single asperity during their loading. Moreover, at a larger nominal surface area of the punch it would difficult or simply impossible to take correct measurements with the profilometer.

As regards the requirements concerning the design of the stand and its measuring capabilities, efforts were concentrated on limiting the effect of the stand structure on the measurement results and on maintaining stable conditions during contact investigations. For this purpose four functions of the device were defined. In order to implement the functions it is necessary to satisfy the requirements described below.

1. **The possibility of supervising the measurement conditions when loading the measuring stand structure.** The aim is to ensure the parallelism of the mutual

approach of the contact surfaces during loading in the normal direction. This was achieved through the measurement of punch inclination relative to the table and ensuring loading in the normal direction through the proper guidance of the movable member in the stand structure. In the design of the structure attention was focused on the way of transmitting the force to the specimen and on the dependencies between the force application point and the displacement measurement points. Thanks to the high precision with which the stand components had been made and assembled most errors were eliminated and replicable device operating conditions as well as the parallelism of the mutual approach of the contact surfaces during loading were ensured.

2. **Protection against an exceedance of the allowable deformation of the load-bearing structure.** Load-bearing structure deformations caused by the torque and the force loading the specimen were considered here. It was estimated that the maximum loading of the load-bearing structure with the torque originating from the manual drive would not exceed 5Nm. For a displacement range of +/-1.5mm the axial force load should not cause any plastic deformations of the device. On the basis of simulations the permissible loading force was determined to be 400N. In order to prevent damage to the force sensors in the case of permissible force value exceedance sensors which can withstand loads of up to 600N were used.
3. **The possibility of loading in the direction normal to the specimen surface.** This condition was satisfied through the selection of specimens characterized by the parallelism of their two surfaces, better than 0.01/10mm, a proper technology of making the punch, the careful setting of its parallelism relative to the table, the special design of the measuring device load-bearing structure and the vacuum fixing of specimens to the table. Moreover, a single fixing was used for the base surface of the punch and the cuboidal component surface, which ensured the parallelism of the planes with an error below 1μm/5mm (0.02/100mm). The base surface of the punch was used to set the latter's parallelism relative to the table surface with an accuracy of +/-0.01/100mm.
4. **The limitation of the influence of the structural components on the behaviour of the load application point-measurement place system.** This was achieved through the minimization of assembly errors and deviations in the chain of dimensions between the punch and the table with the fixed specimen (Fig. 5).

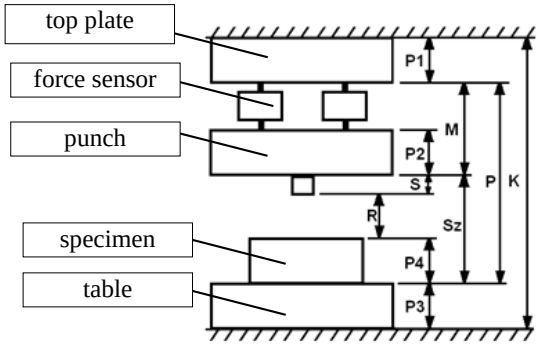

Fig. 5. Chain of dimensions for measuring stand (R=Sz-S-P4 => $\delta_R^2=\delta_{Sz}^2+\delta_s^2+\delta_{P4}^2$)

The variance propagation of mean errors for independent variables was used for error analysis. Three components of punch and specimen surface non-parallelism error (Fig. 5 – δ_R), stemming from the technology of making the measuring stand parts, were optimized whereby dimensional error R was reduced (from δ_R =0.03 to δ_R=0.01mm). The most significant component of error δ_R is the specimen workmanship and fixing error (δ_{P4} – Fig. 5), which ultimately did not exceed 5μm. The vacuum fixing of the specimen contributed to the reduction in the influence of deformations in the specimen-table zone. Another dimensional error component is the base surface and punch contact surface parallelism error (δ_s – Fig. 5). After the measuring stand had been assembled this error did not exceed 5μm/60mm. The last component subjected to optimization related to the assembly of the punch (δ_{Sz} – Fig. 5). The punch together with the force sensors and the plate was attached to the movable member of the load-bearing structure to ensure that the parallelism of its base surface relative to the table was less than 5μm/60mm.

The device has the following distinctive features:

- owing to the movable member design – the member forms a whole with the load bearing structure (Fig. 1b) – its movement in only one direction is guaranteed;
- by adopting a surface contact of 1mm^2 waviness has been eliminated from the measurements, profilometer measurements have been made easier (there is no need to join many images into a single image) and the amount of data needed to build the model, and so the demand for computing power, has been reduced;
- by vacuum fixing the specimen, whereby it can be still moved on the table, one can select any places on the specimen surface to be loaded with the punch;
- since the specimen is not secured to the table, it can be easily retrieved to measure roughness between loadings while the test conditions remain unchanged during the whole test cycle;
- thanks to the measuring stand design the flat-tipped punch can be replaced with punches with other tips without any loss of motion accuracy;
- thanks to the compact design, the number of undesirable elements and links in the chain of dimensions of the measured displacements has been limited.

4. TESTS OF MEASURING STAND

4.1. MEASUREMENTS OF ASPERITY DEFORMATIONS

The deformations of asperities were preliminarily studied for a specimen made of aluminium alloy EN AW-5754, with a milled surface. The specimen profile prior to loading (no. 1 in Fig. 6) was measured and then the specimen was loaded with a force of 150N, which required the displacement of the punch by 12um. After unloading the surface profile was measured again (no. 2 in Fig. 6).

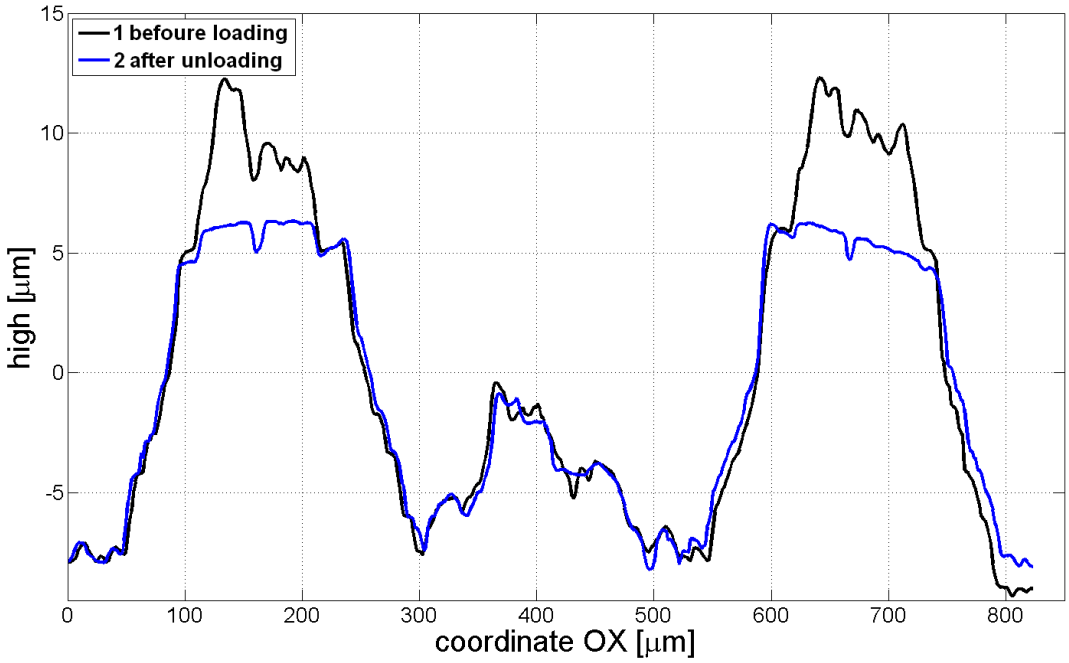

Fig. 6. Comparison of profilograms before loading and after unloading of milled aluminium specimen

The comparison of the two profiles (Fig. 6) shows that the plastic deformation amounted to 6um, which constitutes 29% of the initial value of S_z. In order to confirm this conclusion the graph showing the proximity characteristic of the loaded surfaces (Fig. 7) was used.

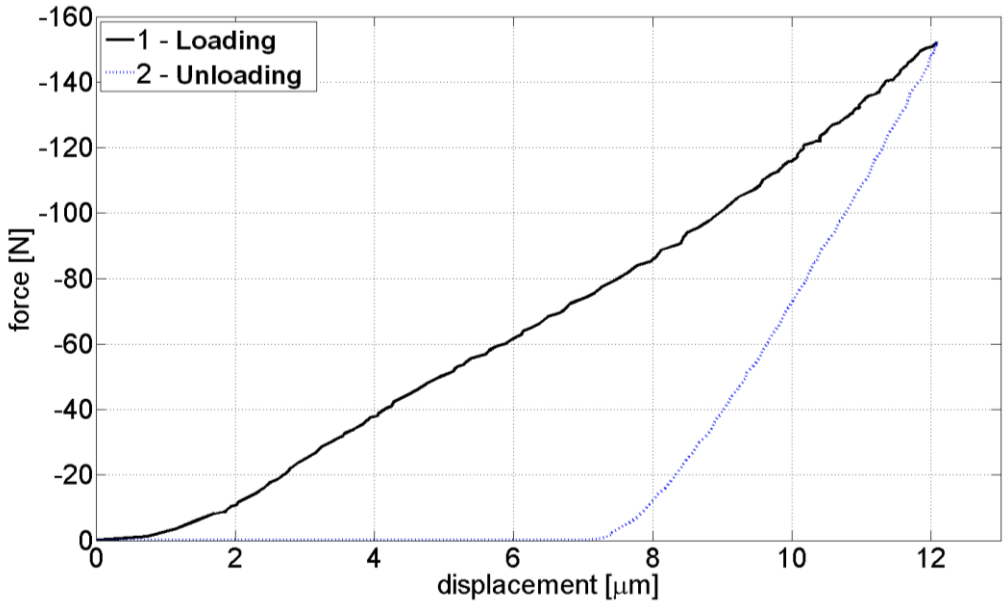

Fig. 7. Mutual approach of contact surfaces for specimen made of aluminium alloy and punch made of quenched steel

The graph shows that the total displacement connected with plastic and elastic deformations under the load of 150N amounted to 12μm. After specimen unloading the share of the displacements due to plastic deformations amounted to 7μm. A comparison of the displacements presented in figs 6 and 7 shows that the difference between the measurements performed using the measuring device (Fig. 7) and the profilogram reading (Fig. 6) amounts to 1μm. This slight difference can be due to the fact that Fig. 6 shows only one of the many profiles in the nominal contact area (Fig. 8). This profile is perpendicular to the machining marks (Fig. 8), which means that it does not take into account changes in the profile along the machining marks.

The features of the device make it possible to study the mutual interactions between microasperities. The results of such analyses depend on the different properties of the investigated contact surfaces. For example, in the case of milled aluminium loaded in the normal direction, by comparing the roughness profiles before and after loading (Fig. 6) one finds that there was no mutual interaction between the microasperities. Three microasperities are visible in the profiles shown in Fig. 6. The two highest microasperities plastically deformed (Fig. 6, line 2) and their deformations did not interact with each other because of the large distance between them. The same applies to the mutual interactions with the lowest microasperity (situated in the middle), as evidenced by no change in the shape of the middle microasperity, which under load (Fig. 6, line no. 1) is the same as after loading (Fig. 6, line 2).

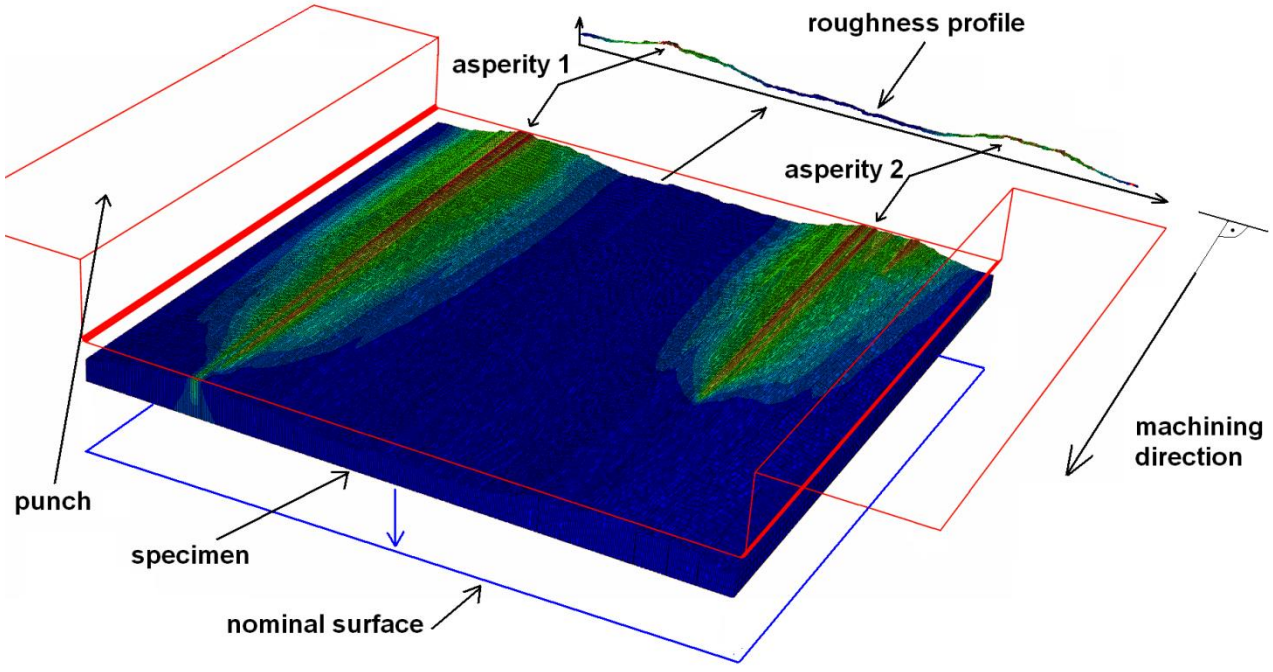

Fig. 8. Asperities visible on specimen surface after loading with normal force

A TalySurf CCILite profilometer was used to measure roughness. An original 2D image with a colour palette would be obtained from the profilometer. The image covers an 0.8x0.8mm area and the colours represent the height of asperities. The original 2D images

with the colour palette were subjected to denoising, levelling and the separation of asperities from waviness. The parameters of the asperities were analyzed using an image with separated roughness.

Having the graph of the mutual approach of the contact surfaces (an exemplary graph is shown in Fig. 7) one can also assess the hypothetical effect of the deformation of asperities on the behaviour of, e.g., a part fixed in a jig. Let us consider such a hypothetical situation using the graph shown in Fig. 7. For example, by fixing a part with a force of 80N one causes the displacement of its surface by about 7µm (a point near the middle of the black line in Fig. 7). When the jigging force is increased to 150N, the displacement increases by further 5µm, whereby the total mutual approach of the surfaces, amounting to 12µm is obtained. When the force loading the contact diminishes, the displacement of the observed surface will decrease consistently with the blue line (Fig. 7). This means that the surfaces being in contact move apart to the position which they occupied prior to overloading, i.e. about 5µm, and the jigging force amounts to close 0N. Thus as a result of the deformation of asperities, caused by contact overloading the workpiece will not be fixed.

4.2. CHECK OF SPECIMEN LOADING PUNCH INCLINATION RELATIVE TO TABLE UNDER SINGLE CONTACT LOADING

While performing measurements on the stand one can observe how large the inclination of the rough surfaces is. This can be done on the basis of four proximity graphs plotted for the four pairs of force-displacement sensors. In the determination of inclination the displacement measurement is more important than the force measurement. For this reason inclination was defined as the maximum value of the scatter of displacement sensor indications. Figure 9 shows the measured proximity characteristics for each of the four pairs of sensors for the milled aluminium specimen subjected to single loading and unloading.

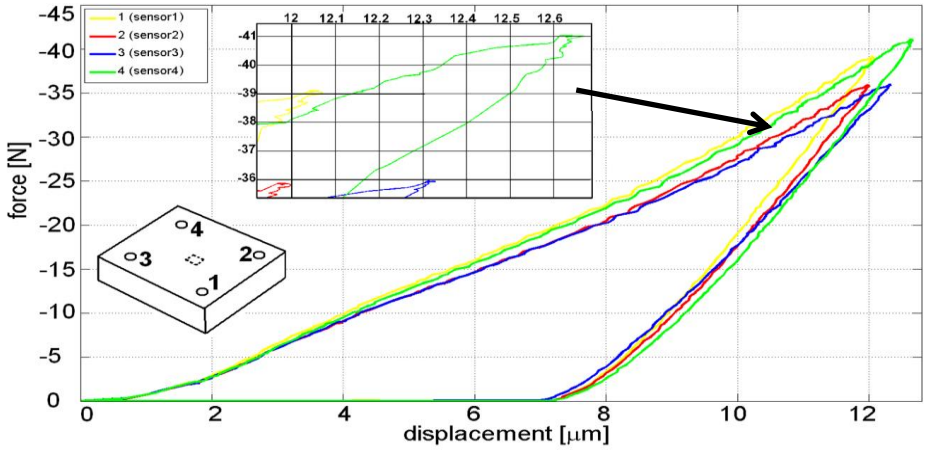

Fig. 9. Sensor indications during single loading and unloading of milled specimen made of aluminium alloy

In the considered case, the scatter of results for all the sensors is not larger than 0.7+/-0.15μm (6% of the maximum displacement) and 5+/-0.05N, (12% of the maximum displacement). The inclination of the punch relative to the specimen, calculated on the basis of the measurements, taking into account the spacing of the displacement sensors, amounted to 0.7μm/60mm.

Similar proximity characteristics were determined for a milled steel specimen subjected to single loading and unloading (Fig. 10). In this case, the maximum scatter of proximity sensor indications did not exceed 1+/-0.15μm (14% of the maximum displacement) and 12+/-0.05N (15% of the maximum displacement).

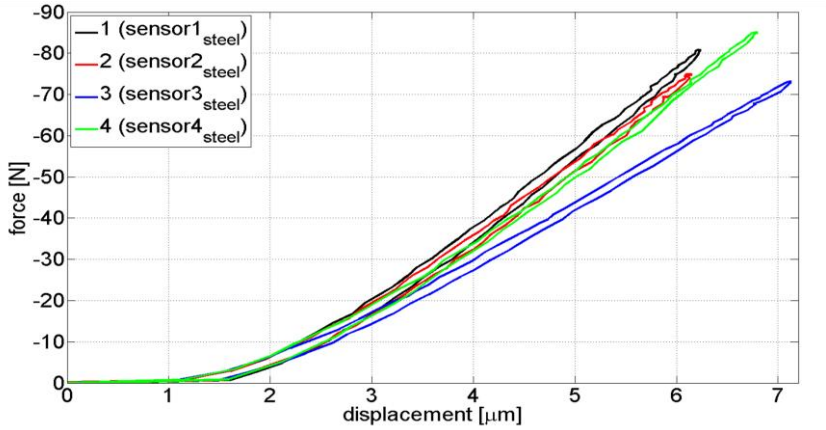

Fig. 10. Sensor indications during single loading and unloading of milled steel specimen

The results of obtained for the milled steel specimen subjected to triple loading and unloading (Fig. 11) are evidence of the high stability of the measuring stand. The good agreement between the characteristics, determined on the basis of the force and displacement measurements in four points distant from one another, shows that the direction of load action was close to the normal direction and the mutual inclinations of the stand components were not significant enough to affect the correctness of the analysis of the proximity characteristics. Also the share of plastic deformations after triple loading for the complete deformation of the contact was determined from the diagrams shown in Fig. 11. The share is not larger than 1μm and the hysteresis does not exceed 5N and 0.2μm.

According to the Dolbey and Bell studies [2], for the cast iron/cast iron contact (after grinding) the load of 0.5N/mm^2 causes a deformation of 1.5um. Whereas the present authors' studies show (Fig. 11) that the deformation of 1.5um is produced by the load of 5N/mm^2 and about 3N/mm^2 is required in the next loading. Even in the case of contact with a milled soft aluminium specimen, a load of about 2N/mm^2 is needed to produce a deformation of 1.5um (Fig. 9). However the authors' results cannot be compared with the Dolbey and Bell results [2]mainly because of the different contact surface areas. In the Dolbey and Bell work [2] a large surface area (76mm × 76mm), which must have included a waviness error, was assumed. As the present authors adopted the contact area of 1mm^2, the waviness error can be regarded as insignificant and the measured deformations can be treated as the deformations of flat surface microasperities.

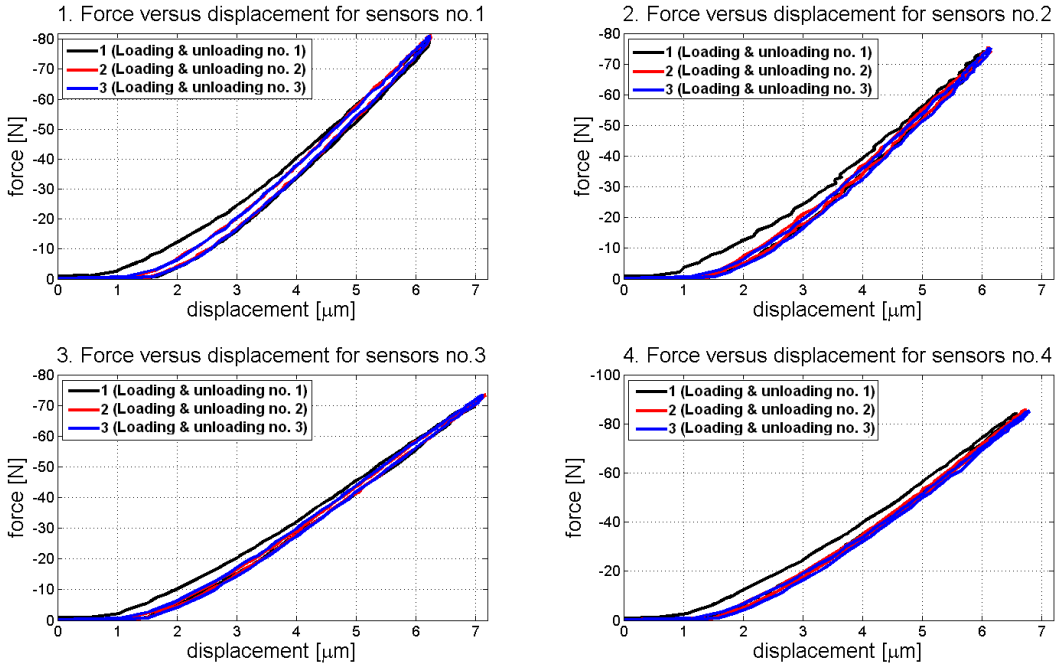

Fig. 11. Proximity characteristics for triple loading and unloading of milled steel specimen for four pairs of force-displacement sensors

4.3. CHECK OF VALIDITY OF SPECIMEN VACUUM FIXING

The proximity characteristics of the fixed and not fixed steel specimen are compared in Fig. 12. In the case of the specimen which was not fixed, a much greater compliance, being the result of the superimposition of the compliance of the investigated contact and the specimen-bottom table contact, was observed. In the case of vacuum fixing, the stiffness of the specimen-table contact is considerably increased whereby more reliable measurement results can be obtained.

4.4. ANALYSIS OF LOAD-BEARING STRUCTURE

The analysis of the load-bearing structure was aided with a computer simulation in which three types of loading which can have a bearing on the deformations of the whole structure, i.e. the force consistent with the normal direction, the force inconsistent with the normal direction and the torque, were taken into account. The first of the cases is tantamount to the application of the force in the symmetry axis of the device cross section. The displacement of the movable member by 1.5mm requires the application of a force amounting to 70N (Fig. 13). During the computer simulation the whole structure of the frame was fixed in the bottom holes whereby displacements could take place only along the axis of the holes. After discretization the model was characterized by:

- the total number of nodes: 200947,
- the total number of elements: 41703,
- 41227 quadratic hexahedral elements of type C3D20R,
- 476 quadratic wedge elements of type C3D15,
- 2 MPCs (the beam).

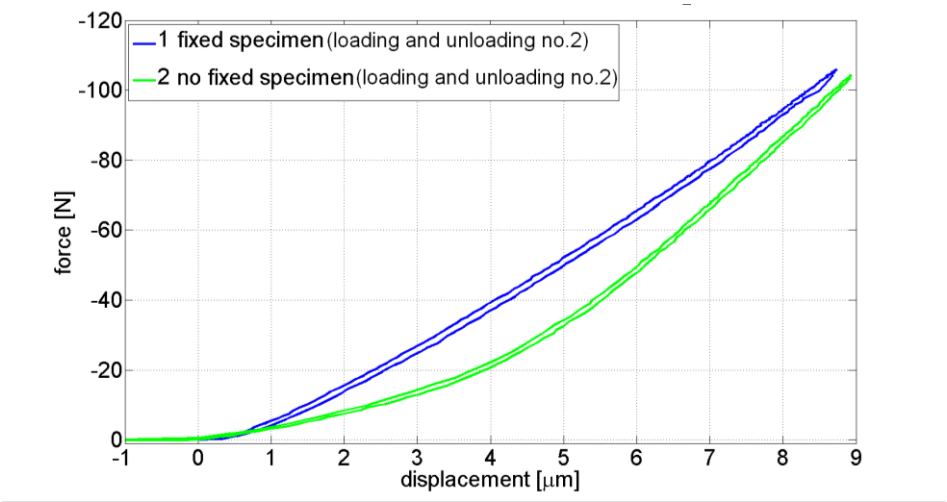

Fig. 12. Comparison of results for not fixed and vacuum fixed steel specimen

Figure 13 shows the behaviour of the most strained member of the load-bearing structure when the movable internal member is loaded with a normal force of 70N. The movable internal member is symmetrically fixed to four 0.5mm thick elastic members (two at the top and two at the bottom).

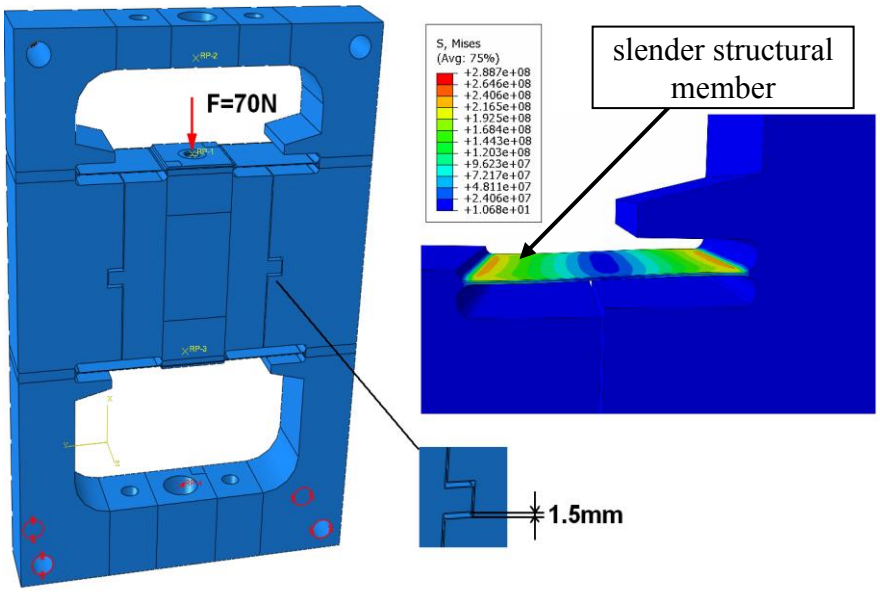

Fig. 13. Stresses in thinnest members of load-bearing structure during displacement of movable member relative to structure by 1.5mm

One of the elastic members in the state of stress is shown in Fig. 13. The reduced stresses determined through the simulation do not exceed 288.7MPa, which means that the structure works in the plastic range. The load-bearing structure has a structural safeguard preventing the accidental exceedance of the displacement of +/-1.5mm, which means that the further increasing of the axial force does not result in a significant increase in stress in the sensitive members.

Also the behaviour of the load-bearing structure under the force of 400N inconsistent with the normal direction was tested. The loads and the results of the computations are shown in Fig. 14. Since the force was applied in the most disadvantageous place one can assume that the computed displacements are maximal. The largest computed displacement in this case amounts to about 7µm. In the physical tests no such maximal displacements were observed, which shows that the preventive measures taken during the design, production and assembly are effective.

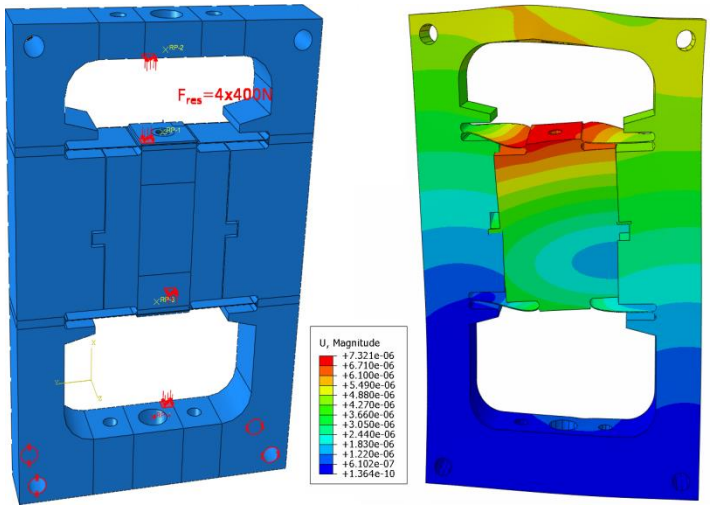

Fig. 14. Boundary conditions and computed displacements for load-bearing structure nonaxially loaded with force of 400N

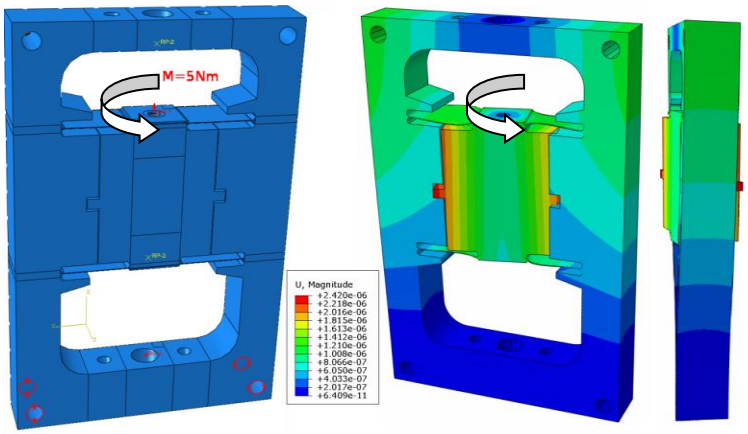

Fig. 15. Boundary conditions and computed displacements for load-bearing structure loaded with torque of 5Nm

Another considered case of load which could occur during the service life of the measuring stand was the loading with a torque moment acting in the point where the screw was fixed. Figure 15 shows the behaviour of the load-bearing structure under the applied torque of 5Nm, twisting the movable internal member. The value of the torque was determined experimentally by making the drive system rotate by means of a torque spanner. As one can see, as a result of loading the load-bearing structure with this torque the structure displaces by max. 2.4μm. It was experimentally determined that the actual torque moments applied to the nut did not exceed 2Nm. Therefore it can stated that the structure performs its function well.

5. CONCLUSION

An original measuring stand, which owing to the small surface area (1mm^2) of its punch enables one to determine the proximity characteristics of even single asperities, has been built. The stand makes it possible to take into account the mutual interactions between individual asperities, which can be of great significance for the quality of the verification of models describing the phenomena occurring at the contact between flat surfaces. A major feature of the stand is that the deviations of the loading direction from the normal direction can be controlled by tracking the punch inclination relative to the table surface by means of four displacement sensors. On the basis of the preliminary studies and analyses one say that the presented measuring stand is characterized by satisfactory stiffness and measuring capabilities adequate for the investigation of contact stiffness characteristics.

The aim of further research will be to create a universal contact model based on selected surface geometric parameters and the device presented here will be used for its verification.

ACKNOWLEDGEMENTS

The investigation have been carried out as part of the project WIPO ***INNOTECH-K1/IN1/75/155671/NCBR/13*** *funded by the Polish National Center for Reasearch and Development (NCBiR). The measurements by means of theTalySurf CCILite (Taylor Hobson) profilometer were carried out in the Laboratory of Mechatronics and Machine Vision, Institute of Production Engineering and Automation, Wroclaw University of Technology. Calculations have been carried out in Wroclaw Centre for Networking and Supercomputing (http://www.wcss.pl), grant No.109.*

REFERENCE

[1] ITO Y., 2008, *Modular design for machine tools*, The McGraw-Hill Companies, Inc., USA, ISBN: 9780071496605.
[2] DOLBEY M. P., BELL R., 1971, *The contact stiffness of joints at low apparent interface pressures* , Annals of the C.I.R.P, XVIV, 67-79.
[3] THORNLEY R., CONNOLLY R., BARASH M., KOENIGSBERGERS F., 1965, *The effect of surface topography*

upon the static stiffness of machine tools joints, International Journal of Machine Tool Design and Research, 5/1-2, 57-74.
[4] SUŁEK M.W., JEDYNAK H.R., 2004, *The effect of the action of plastic asperities on motion resistances at dry friction, Tribologia,* 4, 229-236, (in Polish).
[5] STUPKIEWICZ S., 2007, *Micromechanics of contact and interphase layers, Springer*, Berlin,
[6] SADOWSKI P., STUPKIEWICZ S., 2010, *A model of thermal contact conductance at high real contact area fractions*, Wear, Elsevier, 261/1-2, 77-85.
[7] HOLMBERG K, RONKAINEN H, LAUKKANEN A, WALLIN K., 2007, *Friction and wear of coated surfaces—scales, modelling and simulation of tribomechanisms*, Surface & Coatings Technology, 202/4-7, 1034–1049.
[8] JOHNSON K.L., 1995, *Contact mechanics and the wear of metals,* Wear, 190/2, 162-170.
[9] NOGUEIRA I., ROBBE-VALLOIRE F., GRAS R., 2010, *Experimental validations of elastic to plastic asperity-based models using normal indentations of rough surfaces*, Wear 269, 709–718.
[10] YEAU-REN J., SHIN-RUNG P., 2007, *Contact behaviour of surfaces containing elliptical asperities with gaussian and non-gaussian height distribution,* J Tribol, 129/4, 743-753.
[11] BUCZKOWSKI R., KLEIBER M., 2006, *Elasto-plastic statistical model of strongly anisotropic rough surfaces for finite element 3D-contact analysis*, Computer Methods in Applied Mechanics and Engineering, 195/37–40, 5141–5161.
[12] LIOU J.L., LIN J.F., 2009, *A microcontact model developed* for asperity heights with a variable profile fractal *dimension*, *a surface fractal dimension, topothesy*, *and Non-Gaussian Distribution*, Journal of Mechanics, 25, 103-115.
[13] KUCHARSKI S., STARZYNSKI G., 2014, *Study of contact of rough surfaces, Modelling and experiment*, Wear, 311, 167–179.
[14] PEI L., HYUN S., MOLINARI J.F., ROBBINS ., 2005, *Finite element modelling of elasto-plastic contact between rough surfaces*, Journal of the Mechanics and Physics of Solids, 53/11, 2385–2409.
[15] SELLGREN U., BJÖRKLUND S., ANDERSSONS., 2003, *A finite element-based model of normal contact between rough surfaces*, Wear, 254/11, 1180–1188.
[16] SADOWSKI P., 2008, *The modelling of the heat flow through the surface of contact between rough bodies in plastic working processes,* PhD dissertation, PAN, IPPT, Warsaw, (in Polish).
[17] GROCHOWSKI M., JEDRZEJEWSKI J., 2008, *Comparison of two fea-based approaches in prediction of workpiece-fixture static behaviour*, Journal of Machine Engineering, 8/3, 54-65.
[18] XIONG C.H., WANG MY., YONG T., XIONG Y.L., 2005, *On the prediction of passive contact forces of workpiece-fixture systems*, Proceedings of the Institution of Mechanical Engineer, 219/3, 309-324.